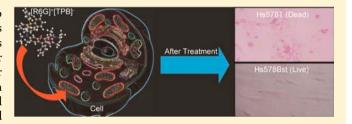# Tunable Cytotoxicity of Rhodamine 6G via Anion Variations

Paul K. S. Magut,[†] Susmita Das,[†] Vivian E. Fernand,[‡] Jack Losso,[§] Karen McDonough,[¶] Brittni M. Naylor,[†] Sita Aggarwal,[∥] and Isiah M. Warner*,[†]

[†]Department of Chemistry, Louisiana State University, Baton Rouge, Louisiana 70803, United States

S *Supporting Information*

ABSTRACT: Chemotherapeutic agents with low toxicity to normal tissues are a major goal in cancer research. In this regard, the therapeutic activities of cationic dyes, such as rhodamine 6G, toward cancer cells have been studied for decades with observed toxicities toward normal and cancer cells. Herein, we report rhodamine 6G-based organic salts with varying counteranions that are stable under physiological conditions, display excellent fluorescence photostability, and more importantly have tunable chemotherapeutic properties.

Our *in vitro* studies indicate that the hydrophobic compounds of this series allow production of nanoparticles which are nontoxic to normal cells and toxic to cancer cells. Furthermore, the anions, in combination with cations such as sodium, were observed to be nontoxic to both normal and cancer cells. To the best of our knowledge, this is the first demonstration that both the cation and anion play an extremely important and cooperative role in the antitumor properties of these compounds.

■ INTRODUCTION

There has recently been tremendous growth in the number of compounds developed as chemotherapeutic agents for treatment of cancer. However, two major obstacles are relevant for chemotherapeutic agents: toxicity toward normal cells and drug resistance. Cationic compounds and multilamellar vesicles with positive charges have been vigorously investigated for this purpose.[1−4] For example, cationic rhodamine dyes have been demonstrated to be good candidates for this line of research, and a number of reports exist dating back to as early as the 1970s.[5−8] Most of these studies suggest that cationic compounds accumulate in the mitochondria of tumor cells due to the unusually high negative mitochondrial membrane potential of tumor cells as compared to normal cells. Upon accumulation and subsequent retention, cationic compounds lead to disruption of adenosine triphosphate (ATP) synthesis in the mitochondria, which eliminates the power source of these cells.[6,7] Other investigations suggest that only the cationic dyes with delocalized positive charge show mitochondrial selectivity[7−9] with little or no focus on the role played by the counteranion. For example, Lampidis and co-workers have performed some very thorough and impressive research on the toxicity of cationic compounds.[10−13] In one of these studies, they report the selective toxicity of cationic rhodamine analogues (rhodamine 123 and 6G), tetraphenyl phosphonium (TTP+), and safranin O toward breast cancer cell line MCF7 in comparison to the normal monkey kidney cell line (CV-1).[6] However, later studies with matched pairs of normal and breast cancer cell lines revealed that rhodamine 123 has no preferential retention or toxicity toward either of these cell lines. Thus, the selectivity reported earlier was attributed to drug resistance caused by a multidrug resistance (*mdr-1*) gene apparently found in the CV-1 cell line but absent in normal and

breast cancer cell lines.[10] It is with these findings in mind that we chose to investigate the effect of counteranions on the antitumor activity of rhodamine 6G to examine if such a change may impart selectivity, particularly towards matched normal and breast cancer cell lines. These anion variations also led to synthesis of organic nanoparticles from the more hydrophobic compounds as discussed later.

Our interest in organic nanoparticles is driven by the significant attention this area has drawn among researchers in the recent past.[14−18] In addition, many types of organic nanoparticles have the advantage of ease of tunability which allows potential applications in varied fields such as optoelectronics, bioimaging, and optical data storage.[17,19−23] The high load of fluorophores in molecular assemblies within nanoparticles is one property that makes them particularly attractive for biomedical applications.[24] With regard to cancer cells, it has been proposed that nanoparticles can achieve increased intracellular concentration, while achieving minimal toxicity in normal cells.[25] Consequently, many recent advances in cancer research to address toxicity of chemotherapeutic agents toward normal cells have led to exploitation of nanoparticles.[26]

Relative hydrophobicity has been shown to influence drug uptake and subcellular distribution of chemotherapeutic agents.[27] To this end, many approaches to varying the hydrophobicity of potential anticancer drugs, especially cationic compounds, involve addition of new groups via covalent bonding or increasing alkyl chain lengths that leads to tedious synthesis of new organic compounds with a primary focus on the contributions of the cation to their anticancer properties.[27]

In the study outlined in this manuscript, we sought to minimize structural differences from the cationic precursors by investigating the effect of the anion on the hydrophobicity and antitumor properties of these compounds *in vitro*. To achieve this goal, we have employed a much simpler strategy to developing compounds with varying hydrophobicities using the concept of variations in hydrophobicity employed for ionic liquids (ILs).[28] In this approach, the cationic dye of choice is held constant while organic counteranions of varying sizes and lipophilic properties are coupled via simple ion-exchange procedures.[20] These compounds are derived from a new class of compounds referred to as a group of uniform materials based on organic salts (GUMBOS). GUMBOS are typically solids which possess many of the attractive properties of ILs.[29] Although GUMBOS share properties similar to those of ILs, these solids are defined as having melting points ranging from 25 to 250 °C, thus broadening the tunable hydrophobic and melting point ranges for select designer materials applications. Additionally, as hydrophobicity increases, water insoluble nanoparticles known as nanoGUMBOS can be fabricated from GUMBOS.[16,20,30] Recently, using a similar concept for solubility of organic compounds in water, Kasai and co-workers have fabricated nanodrugs with anticancer properties from camptothecin derivatives that are insoluble in water.[14]

In this study, we have used the traditionally measured 1-octanol/water partition coefficients to gauge the relative hydrophobicity of these compounds.[31] On the basis of this measure of hydrophobicity, cell viability results revealed that nanoGUMBOS synthesized from hydrophobic GUMBOS are nontoxic to normal cells and toxic to cancer cells while rhodamine 6G chloride and the hydrophilic GUMBOS inhibited cell proliferation for both normal and cancer cells *in vitro*. The anions in combination with sodium or lithium ions were nontoxic to both normal and cancer cells. In the studies introduced in this paper, we demonstrate that both the cation and anion play an active and cooperative role in the observed cytotoxic properties. To the best of our knowledge, this study is the first of its kind. Furthermore, we believe that this approach may be a general one and that this discovery may be of great significance in medicinal chemistry, cancer therapy, and fluorescence bioimaging.

■ RESULTS AND DISCUSSION

Physical and Morphological Properties. Rhodamine 6G-based GUMBOS (Scheme 1) displayed variable physical properties based upon changes in the anion type and size. It was observed that changing the anion affected the melting points of the GUMBOS (Table S1, Supporting Information), as is commonly observed in other low-melting ionic salts such as ionic liquids due to attenuation of crystal packing by larger anions in such salts.[32,33]

NanoGUMBOS from rhodamine 6G tetraphenyl borate ([R6G][TPB]) and rhodamine 6G bis(perfluoroethylsulfonyl) imide ([R6G][BETI]) were primarily spherical or slightly ovate as characterized by use of transmission electron microscopy (TEM) (Figure 1) with an average size of approximately 100 nm. We note that the polydispersity index obtained for these nanoGUMBOS by use of dynamic light scattering (DLS) was generally good, usually under 0.2. The agglomeration observed in Figure 1a may be the result of evaporation of the dispersant.

One (1)-octanol/water partition coefficients were determined in order to gauge the relative hydrophobicities of the synthesized compounds[34,35] Trends beginning with least

Scheme 1. Synthesis of (a) Hydrophobic and (b) Hydrophilic R6G-Based GUMBOS
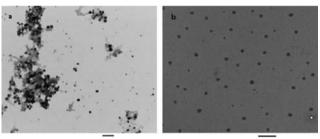

Figure 1. NanoGUMBOS TEM micrographs of (a) [R6G][TPB] size: 92 ± 17 nm and (b) [R6G][BETI] size: 101 ± 21 nm. Scale bars represent 500 nm.

hydrophobic were rhodamine 6G ascorbate ([R6G][Asc]) < rhodamine 6G trifluoromethanesulfonate ([R6G][OTf]) < [R6G][TPB] < [R6G][BETI] (Table S1, Supporting Information). These observed variations in partition coefficients clearly demonstrate that anions play an important role in determining hydrophobicities of [R6G]-based organic salts. Dissociation constants of rhodamine 6G-based GUMBOS were also determined (Table S2, Supporting Information), and observed trends were very consistent with our measured octanol/water partition coefficients. Compared to [R6G][Cl], [R6G][BETI] and [R6G][TPB] show very low dissociation constants, while [R6G][OTf] and [R6G][Asc] show moderate dissociation constants, which underscores the role played by anions in tuning this physical property of GUMBOS. [R6G][BETI] has dissociation constants of 1.35×10^{-12} and 7.36×10^{-12} and [R6G][TPB] has values of 1.37×10^{-11} and 1.52×10^{-11} in pH 6.5 and pH 7.4 buffer solutions, respectively. The low values of dissociation constants of [R6G][BETI] and [R6G][TPB] in PBS solutions suggest that these two GUMBOS are very insoluble in PBS solution, where they form nanoGUMBOS. This study also demonstrates that pH is an important factor for evaluating solubility of rhodamine 6G-based GUMBOS. Generally, lower pH values favor less dissociated GUMBOS.

Absorption and Fluorescence Studies. Ethanolic solutions of [R6G]-based GUMBOS displayed essentially identical absorption spectra with values of λ_{max} near 525 nm,

which were similar to the precursor, [R6G][Cl] (Figure S1a, Supporting Information). Use of these compounds in biological systems requires investigations of their spectral behavior at physiological pH. In phosphate buffered saline (PBS, pH= 7.4, ionic strength, I = 0.15 M), [R6G][TPB] and [R6G][BETI] nanoGUMBOS exhibited broad absorption spectra with a shoulder in the red region relative to the peak maxima (Figure S1b, Supporting Information).

The deconvoluted absorption spectra (inset of Figure S1b, Supporting Information) of [R6G][TPB] and [R6G][BETI] nanoGUMBOS reveal that each absorption spectrum can be decomposed into two major bands attributed to two different types of absorbing species.[16] The spectral component absorbing at ~525 nm is assigned to aggregates within the dye nanoGUMBOS with transition dipoles that are often randomly oriented in dilute solutions.[36] The red-shifted spectral component is attributed to J-type aggregation in which the transition dipoles are arranged in a staircase manner.[37] Although J-aggregation is expected to lead to narrowing of the spectral line, the absorption profile for our nanoGUMBOS is relatively broader. This broadening may be attributed to imperfect J-aggregation, lack of motional narrowing, or the presence of lattice disorder within nanoGUMBOS.[38,39] The more hydrophilic GUMBOS, [R6G][Asc] and [R6G][OTf], displayed absorbance profiles similar to [R6G][Cl], possibly due to similar solubility in water.

An intense fluorescence emission signal from nanoGUMBOS appears near 550 nm with the fluorescence excitation and emission spectra following the expected mirror-image rule as a result of Franck–Condon factors (Figure S2a, Supporting Information). We determined the quantum yields of the [R6G]-based GUMBOS via a previously reported comparative method,[40] using [R6G][Cl] as the standard.[41] In addition, we have determined the lifetimes of these compounds (Table S3, Supporting Information). Evaluation of results showed minimal differences in quantum yields and lifetimes with changes in the anion. This implies that fluorescence properties of these compounds are strongly influenced by properties of the cationic fluorophore and are minimally affected by the anions. This feature allowed the fluorescence properties of the R6G moiety to be essentially maintained, while tuning other physical properties of GUMBOS. Intrinsic photostability was also monitored to evaluate the molecular response of the GUMBOS and nanoGUMBOS upon exposure to light. Evaluation of data from these studies revealed excellent photostability with [R6G][TPB] being the most photostable. It was observed that signal retention ranged from 62% to 90% after 5000 s of irradiation (Figure S2b, Supporting Information), which suggests relatively long shelf life if these materials were to be developed as drug or imaging contrast agents.

Stability of [R6G]-Based NanoGUMBOS. Colloidal stabilities of nanoGUMBOS in phosphate-buffered saline (PBS, pH= 7.4, ionic strength, I = 0.15 M) and serum-PBS (10% serum in PBS) were investigated by monitoring absorbance at λ = 530 nm and emission at λ = 550 nm over a 48 h period. We observed a gradual decrease in the relative absorbance and emission when nanoGUMBOS were dispersed in PBS (Figure 2a).

This decrease in signal is partly attributed to adsorption of nanoGUMBOS on the walls of the glass vial in which they were prepared.[42] Attenuation of intensities may also be a result of nanoparticle aggregation or reorientation with time. It is interesting to note that we observed an increase in absorbance
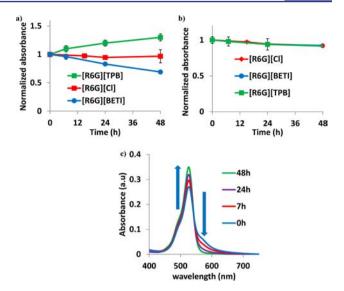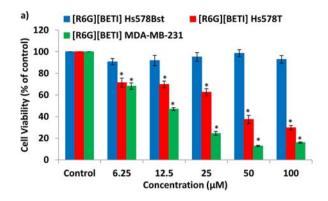

Figure 2. Stability of nanoGUMBOS in (a) PBS, (b) 10% serum, and (c) absorbance spectra corresponding to [R6G][TPB] in PBS showing transition from J-aggregates (λ = 582 nm) to randomly oriented aggregates (λ = 525 nm).

(Figure 2a) and fluorescence emission for [R6G][TPB] nanoGUMBOS in PBS, which is attributed to dye deaggregation over time. This was confirmed by monitoring the absorption spectra as depicted in Figure 2c where the peak earlier attributed to J-aggregates (λ = 582 nm) for [R6G][TPB] nanoGUMBOS decreased in absorbance with time as the one attributed to randomly oriented aggregates (λ = 525 nm) increased. This suggests a gradual shift from the more ordered J-aggregates to randomly oriented aggregates in PBS. In contrast, when nanoGUMBOS were dispersed in serum-PBS, little or no changes in absorption intensity (Figure 2b) and fluorescence emission were observed. This is likely due to prevention of nonspecific adsorption to the walls of the glass vials by serum proteins. This observation is consistent with previous literature where bovine serum albumin was used to prevent nonspecific adsorption of PEGylated gold nanoparticles.[42] This study of nanoGUMBOS in serum-PBS suggests a possible fate of these materials if used in vivo. Thus, their extraordinary stability enhances their potential for such applications.

Cell Studies. MTT assay was used as the primary method for evaluating cytotoxicities, while microscopy was used to corroborate these findings. Initial studies were performed using a suspension of hydrophobic GUMBOS in PBS. After examining these suspensions, we observed the presence of micro- and nanoparticles (Figure S3, Supporting Information). Therefore, further studies were performed by synthesis of nanoGUMBOS with an average size of approximately 100 nm from hydrophobic [R6G][BETI] and [R6G][TPB]. This ensured uniformity in the size of the nanoGUMBOS. Various cell lines were treated with varying concentrations of nanoGUMBOS and it was observed that viability of the normal breast cell line remained largely unaffected, while breast cancer cell proliferation was inhibited in a concentration dependent manner (Figure 3). The MTT assay results were consistent with light microscopy images acquired after 48h treatment of the cells with [R6G][BETI] and [R6G][TPB] (Figure 4). At the end of 48 h, it was observed that the normal breast cell line (HS578Bst) appeared attached firmly and healthy. In contrast,
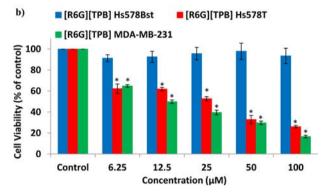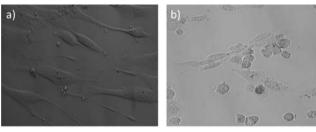
Figure 3. Cell viability assay of Hs578Bst, Hs578T, and MDA-MB-231 cell lines upon treatment with (a) [R6G][BETI] and (b) [R6G]-[TPB]. *Statistically different from control, $P < 0.0001$.
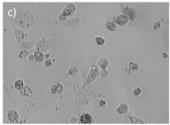

Figure 4. Light microscopy images of (a) normal breast cell line Hs578Bst and breast cancer cell lines (b) Hs578T and (c) MDA-MB-231 after treatment with 50 μM [R6G][TPB] for 48 h. Cell images were obtained using a light microscope equipped with a camera at a magnification of 20×.

the breast cancer cell lines (Hs578T and MDA-MB-231) appeared smaller, round up and detached consistent with the morphology observed when adherent cells die. It is also interesting to note that these compounds were found to be more toxic toward more aggressive and invasive cancer cell lines than toward less invasive cell lines. For example, the IC$_{50}$ values for the more invasive and aggressive MDA-MB-231 were 11.4 and 12.2 μM for [R6G][BETI] and [R6G][TPB] respectively, while it was >100 μM for the noninvasive MCF7 (Table S4 and

Figure S4, Supporting Information). In contrast, the hydrophilic [R6G][OTf] and [R6G][Asc] inhibited cell proliferation of both normal and breast cancer cell lines.

A summary of the IC$_{50}$ values is displayed in Table S4 (Supporting Information). Using control experiments, it was observed that the cation, rhodamine 6G, inhibited cell proliferation of both normal and breast cancer cell lines in agreement with previous literature,[6] while the anions [Li]-[BETI] and [Na][TPB] were not observed to have a significant effect on any of the investigated cell lines (Figure S5, Supporting Information). This definitively demonstrates that the cation and anion combination plays an active and cooperative role in the observed selective properties, particularly for hydrophobic compounds. Apoptosis was identified as the mode of cell death using a Cell death ELISA kit (Figure S6, Supporting Information). In addition, clonogenic assay revealed that [R6G][BETI] and [R6G][TPB] prevented colony formation of cancer cell lines when surviving cells were cultured after treatment with a low dosage of these two compounds (Figure S7, Supporting Information). Thus, these compounds may be good candidates for further investigations as possible chemotherapeutic agents.

Uptake of nanoparticles by individual cells is usually mediated by either nonspecific or specific receptor interactions, commonly via endocytosis. The charge, hydrophobicity, and size of nanoparticles greatly influence this cellular uptake.[43,44] The [R6G][BETI] and [R6G][TPB] nanoparticles displayed a net negative surface charge as gauged by measurement of their zeta potentials. This charge was pH dependent, becoming more negative at physiological pH and less negative at acidic pH. Breast cancer cell lines have been found to have acidic extracellular pH ($\sim$6.5)[45] in comparison to normal cells ($\sim$7.4).[46] From our results, at pH 6.5 the zeta potential of [R6G][BETI] and [R6G][TPB] were −10 and −8 mV, respectively, while at pH 7.4 they were −16 and −18 mV, respectively (Table 1). Since the cell membrane is negatively

Table 1. Zeta Potentials of [R6G][BETI] and [R6G][TPB] NanoGUMBOS

nanoGUMBOS	pH	zeta potential (mV)
[R6G][BETI]	6.5	−9.9 ± 0.9
[R6G][BETI]	7.4	−16.2 ± 1.2
[R6G][TPB]	6.5	−8.0 ± 0.9
[R6G][TPB]	7.4	−17.8 ± 1.5

charged,[27] it is reasonable to expect that at pH 7.4, electrostatic repulsion between the nanoparticles (with high negative charge at this pH) and the cell membrane may lead to reduced uptake in normal breast cells. At lower values of pH, however, repulsive forces are reduced since nanoGUMBOS possess less net negative surface charge and thus may have greater uptake in cancer cell lines.

This uptake may be further enhanced via hydrophobic interactions with cancer cell membranes. This conclusion is supported by cellular uptake data in which MDA-MB-231 displayed higher mean fluorescence intensities, in comparison to Hs578Bst, when the two cell lines were treated with the same concentrations of [R6G][BETI] and [R6G][TPB] nanoGUMBOS (Figure 5). Furthermore, the acidity of the extracellular pH value in cancer cells is primarily due to production of lactic acid, a consequence of increased glycolytic activity. This acidity is proportional to the number of cells as
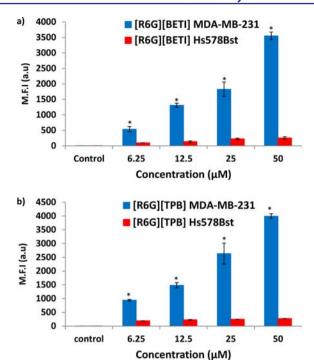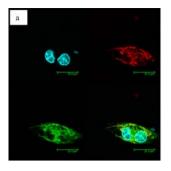
15876

dx.doi.org/10.1021/ja407164w | J. Am. Chem. Soc. 2013, 135, 15873–15879

Figure 5. Mean fluorescence intensity (MFI) of breast cancer cell line MDA-MB-231 (blue) and normal breast cell line Hs578Bst (red) treated with (a) [R6G][BETI] and (b) [R6G][TPB]. *Statistically different from corresponding concentration in Hs578Bst for the same compound ($P < 0.0001$).

Figure 6. Confocal microscopy analysis of (a) [R6G][BETI] and (b) [R6G][TPB] in MDA-MB-231. The fluorescent images show the DAPI-labeled nucleus (blue), Mitotracker Deep Red 633-labeled mitochondria (red), [R6G][BETI] or [R6G][TPB] (green), and a merged image that shows the two compounds mainly localize in the mitochondria.

well as aggressiveness of the cell line.[47] For example, MCF7 which is noninvasive and less aggressive has been shown to acidify its extracellular environment to a lower extent in comparison to the more invasive and aggressive MDA-MB-231.[47] This is consistent with our results in which IC_{50} values for MCF7 were above 100 μM for the two compounds, while for MDA-MB-231 they were slightly above 10 μM as previously noted. We investigated this reasoning by conducting uptake experiments in the normal breast cell line at pH 6.5 for various concentrations of nanoGUMBOS. We observed a significant improvement in uptake of at least 2-fold (Figure S8, Supporting Information). However, this improved uptake was still significantly lower (at least an order of magnitude lower) in comparison to uptake in the breast cancer cell lines. This implies that there are other factors contributing to improved uptake in breast cancer cell lines. Studies to elucidate these other factors including possible differences in cell membranes of the various cell lines are ongoing in our laboratory.

By use of confocal microscopy, the NanoGUMBOS were observed to primarily localize in the mitochondria (Figure 6). Thus, it is reasonable to expect that cell death could be a result of inhibition of mitochondrial function since this is the mechanism previously observed for rhodamine 6G.[5,48] This conclusion was examined by use of a Mitochondrial ToxGlo Assay (Promega Corp.) kit, which predicts potential mitochondrial dysfunction upon exposure to various drugs. The kit consists of two major components. The first is a fluorogenic peptide substrate (bis-AAF-R110) which cannot cross membranes of live cells, and hence its fluorescence is proportional to dead cells (cytotoxicity).[49] The second component is an ATP detection reagent. This reagent leads to lysis of viable cells to release ATP and in the process produces a luminescent signal that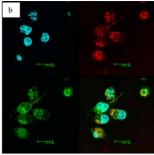 is proportional to the quantity of ATP present. Test compounds that inhibit oxidative phosphorylation lead to a decrease in ATP measured with either no change or discordant changes in cytotoxicity. In contrast, concordant decreases in ATP and increases in cytotoxicity are indicative of primary necrosis and hence are non-mitochondrial. On the basis of our observed results, ATP production was reduced with discordant changes in cytotoxicity of MDA-MB-231 cells exposed to [R6G][BETI] and [R6G][TPB] (Figure S9, Supporting Information), indicating that these two compounds are mitochondrial toxins. Thus, we conclude that toxicity of these two compounds toward breast cancer cell lines result from inhibition of oxidative phosphorylation in the mitochondria of cancer cells as previously reported for rhodamine 6G.[5,48] This conclusion is consistent with the counteranion of rhodamine 6G playing a significant and cooperative role in the selectivity observed in the studies reported in this manuscript.

CONCLUSION

In summary, we have synthesized and investigated the hydrophobic, luminescence, stability, and cellular uptake properties of novel fluorescent GUMBOS. In addition, nanoGUMBOS with an average size of approximately 100 nm in diameter were fabricated by use of a simple, rapid, reproducible, and additive-free reprecipitation method. We have demonstrated tunability of the physicochemical properties of these compounds. Most notably, evaluation of data from this study indicates that both the cation and anion in this class of compounds play an active and cooperative role in the observed selective antitumor cell proliferation potential. This is a remarkable finding since the effect of cationic compounds (particularly rhodamine 6G) on normal and cancer cell lines has been studied for decades with no similar observations. Thus, achieving selective anticancer activity simply by altering the anion of a known anticancer agent such as rhodamine 6G opens new avenues for research and discovery of inexpensive anticancer drugs since the synthetic routes outlined here for production of GUMBOS and nanoGUMBOS are rather simple. A particular interesting aspect of this study is that this may be an approach which is generally applicable to other cationic compounds whose toxicities have been previously studied in detail. Finally, the luminescence properties of these compounds may allow the design of probes that will help to visualize tumor cells for surgical removal while at the same time inducing cell death in residual cancerous tissue.

■ EXPERIMENTAL SECTION

Synthesis of Rhodamine 6G-Based GUMBOS. GUMBOS were synthesized by use of ion-exchange procedures similar to those previously reported in the literature,[20,28] with slight modifications (Scheme 1). Full synthesis and characterization details for the investigated compounds are provided in the Supporting Information.

Synthesis of Rhodamine 6G-Based Nanogumbos. Nano-GUMBOS were synthesized by use of a slightly modified, additive free reprecipitation method.[50] Briefly, 1 mL of 1 mM GUMBOS were prepared by dissolving in DMSO such that the final volume of DMSO was no more than 10% and topped off at the 1 mL mark using cell media (DMEM containing 10% fetal bovine serum), followed by sonication for 5 min. A 100 μL aliquot of this solution was resuspended in 1 mL cell media under sonication to prepare 100 μM of nanoGUMBOS. These nanoGUMBOS were then left to age in the dark for 1 h. For nanoGUMBOS characterization, a few microliters were dropcast onto a carbon-coated copper grid and left to dry at room temperature. Upon drying, the grids were washed several times with water to remove the cell media. A similar protocol was used to synthesize nanoGUMBOS for stability studies with PBS or 10% serum in PBS as the solvent instead of cell media. The average particle size and size distribution of nanoGUMBOS were determined by use of transmission electron microscopy (TEM) using an LVEM5 transmission electron microscope (Delong America, Montreal, Canada) and dynamic light scattering (DLS). The zeta potentials of nanoGUMBOS at various pH values were measured by using a Zetasizer Nano ZS (Malvern Instruments, U.K.).

Absorption and Fluorescence Spectroscopy. UV−vis spectra were collected using a Shimadzu UV-3101 PC UV−vis−near-IR scanning spectrometer (Shimadzu, Columbia, MD). Steady-state fluorescence measurements were recorded at room temperature by use of a Spex Fluorolog-3 spectrofluorimeter (model FL3-22TAU3; Jobin Yvon, Edison, NJ) equipped with a 450 W xenon lamp and R928P photomultiplier tube (PMT) emission detector. A 0.4 cm^2 quartz cuvette (Starna Cells) was used to collect the fluorescence and absorbance relative to an identical cell filled with relevant solvent as the blank. Both normalized and non-normalized absorption spectra were deconvoluted using principal component analysis and fits with lowest $\chi 2$ values were accepted.[16] A two component Gaussian fit was used to deconvolute both the normalized and non-normalized absorption spectra.

Cell Studies. *In vitro* experiments were performed using normal human breast fibroblast (Hs578Bst), human breast carcinoma (Hs578T), hormone-independent human breast adenocarcinoma (MDA-MB-231), and hormone-dependent human breast adenocarcinoma (MCF7) cell lines (ATCC, Manassas, VA). Cytotoxicities of [R6G]-based compounds were determined using an MTT assay kit (Promega Corp., Madison, WI) according to the manufacturer's instructions. Apoptotic cell death was established using a Cell death ELISA assay kit (Roche Applied Sciences, Indianapolis, IN) as per the manufacturer's instruction. Clonogenic assay with MDA-MB-231 was performed according to a procedure described in the literature.[51] Details of all *in vitro* experiments are provided in the Supporting Information.

Statistics. Statistical analyses were performed using one-way analysis of variance (ANOVA). Tukey's studentized range test was performed to ascertain significant differences between treatments within the 95% confidence interval using SAS 9.2 software (SAS, Cary, NC). $P < 0.05$ was considered to indicate statistical significance. Results shown are representative of at least three experiments and are expressed as mean ± SD.

■ ASSOCIATED CONTENT

Ⓢ Supporting Information
Detailed methods, figures, and tables that support the discussions in this manuscript. This material is available free of charge via the Internet at http://pubs.acs.org.

■ AUTHOR INFORMATION

Corresponding Author
iwarner@lsu.edu

Present Addresses
‡(V.E.F.) Department of Chemistry and Physics, LeTourneau University, Longview, TX 75602.
§(J.L.) Department of Food Science, Louisiana State University Baton Rouge, LA 70803.
¶(K.M.) Veterinary Science Department, Louisiana State University, Baton Rouge, LA 70803.
∥(S.A) William Hansel Cancer Prevention, Pennington Biomedical Research Center, Baton Rouge, LA 70808.

Author Contributions
The manuscript was written through contributions of all authors.

Notes
The authors declare no competing financial interest.

■ ACKNOWLEDGMENTS

■ REFERENCES

(1) Kelland, L. *Nature Rev. Cancer* **2007**, *7*, 573.
(2) Kawakami, M.; Koya, K.; Ukai, T.; Tatsuta, N.; Ikegawa, A.; Ogawa, K.; Shishido, T.; Chen, L. B. *J. Med. Chem.* **1998**, *41*, 130.
(3) Abrams, M. J.; Picker, D. H.; Fackler, P. H.; Lock, C. J. L.; Howardlock, H. E.; Faggiani, R.; Teicher, B. A.; Richmond, R. C. *Inorg. Chem.* **1986**, *25*, 3980.
(4) Takaha, N.; Nakanishi, H.; Kimura, Y.; Hongo, F.; Kamoi, K.; Kawauchi, A.; Mizuno, M.; Yoshida, J.; Wakabayashi, T.; Miki, T. *Int. J. Oncol.* **2012**, *40*, 1441.
(5) Gear, A. R. L. *J. Biol. Chem.* **1974**, *249*, 3628.
(6) Lampidis, T. J.; Hasin, Y.; Weiss, M. J.; Chen, L. B. *Biomed. Pharmacother.* **1985**, *39*, 220.
(7) Kurtoglu, M.; Lampidis, T. J. *Mol. Nutr. Food Res.* **2009**, *53*, 68.
(8) Chen, L. B.; Summerhayes, I. C.; Johnson, L. V.; Walsh, M. L.; Bernal, S. D.; Lampidis, T. J. *Cold Spring Harb. Symp. Quant. Biol.* **1982**, *46* (Part 1), 141.
(9) Johnson, L. V.; Walsh, M. L.; Chen, L. B. *Proc. Natl. Acad. Sci., Biol.* **1980**, *77*, 990.
(10) Broutyboye, D.; Kolonias, D.; Wu, C. J.; Savaraj, N.; Lampidis, T. J. *Cancer Res.* **1995**, *55*, 1633.
(11) Hu, Y. P.; Moraes, C. T.; Savaraj, N.; Priebe, W.; Lampidis, T. J. *Biochem. Pharmacol.* **2000**, *60*, 1897.
(12) Lampidis, T. J.; Castello, C.; Delgiglio, A.; Pressman, B. C.; Viallet, P.; Trevorrow, K. W.; Valet, G. K.; Tapiero, H.; Savaraj, N. *Biochem. Pharmacol.* **1989**, *38*, 4267.
(13) Lampidis, T. J.; Planas, L.; Tapiero, H. *Proc. Am. Assoc. Canc. Res.* **1986**, *27*, 397.
(14) Kasai, H.; Murakami, T.; Ikuta, Y.; Koseki, Y.; Baba, K.; Oikawa, H.; Nakanishi, H.; Okada, M.; Shoji, M.; Ueda, M.; Imahori, H.; Hashida, M. *Angew. Chem., Int. Ed.* **2012**, *51*, 10315.
(15) de Rooy, S. L.; El-Zahab, B.; Li, M.; Das, S.; Broering, E.; Chandler, L.; Warner, I. M. *Chem. Commun.* **2011**, *47*, 8916.

(16) Das, S.; Bwambok, D.; Ei-Zahab, B.; Monk, J.; de Rooy, S. L.; Challa, S.; Li, M.; Hung, F. R.; Baker, G. A.; Warner, I. M. *Langmuir* **2010**, *26*, 12867.

(17) Tian, Z.; Wu, W.; Li, A. D. Q. *ChemPhysChem* **2009**, *10*, 2577.

(18) Peng, A. D.; Xiao, D. B.; Ma, Y.; Yang, W. S.; Yao, J. N. *Adv. Mater.* **2005**, *17*, 2070.

(19) Anthony, J. E. *Chem. Rev.* **2006**, *106*, 5028.

(20) Bwambok, D. K.; El-Zahab, B.; Challa, S. K.; Li, M.; Chandler, L.; Baker, G. A.; Warner, I. M. *ACS Nano* **2009**, *3*, 3854.

(21) Park, S.; Kwon, J. E.; Kim, S. H.; Seo, J.; Chung, K.; Park, S.-Y.; Jang, D.-J.; Medina, B. M.; Gierschner, J.; Park, S. Y. *J. Am. Chem. Soc.* **2009**, *131*, 14043.

(22) Yoon, S.-J.; Chung, J. W.; Gierschner, J.; Kim, K. S.; Choi, M.-G.; Kim, D.; Park, S. Y. *J. Am. Chem. Soc.* **2010**, *132*, 13675.

(23) An, B.-K.; Kwon, S.-K.; Park, S. Y. *Angew. Chem., Int. Ed.* **2007**, *46*, 1978.

(24) Breton, M.; Prevel, G.; Audibert, J.-F.; Pansu, R.; Tauc, P.; Le Pioufle, B.; Francais, O.; Fresnais, J.; Berret, J.-F.; Ishow, E. *Phys. Chem. Chem. Phys.* **2011**, *13*, 13268.

(25) Haley, B.; Frenkel, E. *Urol. Oncol. Semin. O. I.* **2008**, *26*, 57.

(26) Cho, K.; Wang, X.; Nie, S.; Chen, Z.; Shin, D. M. *Clin. Cancer Res.* **2008**, *14*, 1310.

(27) Kandela, I. K.; Lee, W.; Indig, G. L. *Biotech. Histochem.* **2003**, *78*, 157.

(28) Fraga-Dubreuil, J.; Famelart, M. H.; Bazureau, J. P. *Org. Process Res. Dev.* **2002**, *6*, 374.

(29) Akdogan, Y.; Junk, M. J. N.; Hinderberger, D. *Biomacromolecules* **2011**, *12*, 1072.

(30) Tesfai, A.; El-Zahab, B.; Kelley, A. T.; Li, M.; Garno, J. C.; Baker, G. A.; Warner, I. M. *Acs Nano* **2009**, *3*, 3244.

(31) Biagi, G. L.; Recanatini, M.; Barbaro, A. M.; Borea, P. A. *Process Control Qual.* **1997**, *10*, 129.

(32) Lopez-Martin, I.; Burello, E.; Davey, P. N.; Seddon, K. R.; Rothenberg, G. *ChemPhysChem* **2007**, *8*, 690.

(33) Larsen, A. S.; Holbrey, J. D.; Tham, F. S.; Reed, C. A. *J. Am. Chem. Soc.* **2000**, *122*, 7264.

(34) Lee, S. H.; Lee, S. B. *J. Chem. Technol. Biotechnol.* **2009**, *84*, 202.

(35) Kamlet, M. J.; Abraham, M. H.; Doherty, R. M.; Taft, R. W. *J. Am. Chem. Soc.* **1984**, *106*, 464.

(36) Kasha, M.; Rawls, H. R.; Ashraf El-Bayoum, M. *Pure Appl. Chem.* **1965**, *11*, 371.

(37) Kumar, V.; Baker, G. A.; Pandey, S. *Chem. Commun.* **2011**, *47*, 4730.

(38) An, B. K.; Kwon, S. K.; Jung, S. D.; Park, S. Y. *J. Am. Chem. Soc.* **2002**, *124*, 14410.

(39) Jelley, E. E. *Nature* **1936**, *138*, 1009.

(40) Williams, A. T. R.; Winfield, S. A.; Miller, J. N. *Analyst* **1983**, *108*, 1067.

(41) Magde, D.; Wong, R.; Seybold, P. G. *Photochem. Photobiol.* **2002**, *75*, 327.

(42) Takae, S.; Akiyama, Y.; Otsuka, H.; Nakamura, T.; Nagasaki, Y.; Kataoka, K. *Biomacromolecules* **2005**, *6*, 818.

(43) Gratton, S. E. A.; Ropp, P. A.; Pohlhaus, P. D.; Luft, J. C.; Madden, V. J.; Napier, M. E.; DeSimone, J. M. *Proc. Natl. Acad. Sci. U.S.A.* **2008**, *105*, 11613.

(44) Sahay, G.; Kim, J. O.; Kabanov, A. V.; Bronich, T. K. *Biomaterials* **2010**, *31*, 923.

(45) Du, J.-Z.; Du, X.-J.; Mao, C.-Q.; Wang, J. *J. Am. Chem. Soc.* **2011**, *133*, 17560.

(46) Zhang, X.; Lin, Y.; Gillies, R. J. *J. Nucl. Med.* **2010**, *51*, 1167.

(47) Montcourrier, P.; Silver, I.; Farnoud, R.; Bird, I.; Rochefort, H. *Clin. Exp. Metastasis* **1997**, *15*, 382.

(48) Darzynkiewicz, Z.; Traganos, F.; Staianocoico, L.; Kapuscinski, J.; Melamed, M. R. *Cancer Res.* **1982**, *42*, 799.

(49) Niles, A. L.; Moravec, R. A.; Hesselberth, P. E.; Scurria, M. A.; Daily, W. J.; Riss, T. L. *Anal. Biochem.* **2007**, *366*, 197.

(50) Kasai, H.; Nalwa, H. S.; Oikawa, H.; Okada, S.; Matsuda, H.; Minami, N.; Kakuta, A.; Ono, K.; Mukoh, A.; Nakanishi, H. *Jpn. J. Appl. Phys., Part 2* **1992**, *31*, L1132.

(51) Franken, N. A. P.; Rodermond, H. M.; Stap, J.; Haveman, J.; van Bree, C. *Nature Protocols* **2006**, *1*, 2315.